Pergamon

Atmospheric Environment Vol. 29, No. 16, pp. 2163–2176, 1995

1352 2310/95 $9.50 + 0.00

1352–2310(94)00241–X

ROLE OF VEGETATION IN GENERATION OF MESOSCALE CIRCULATION

XIAODONG HONG, MARTIN J. LEACH and SETHU RAMAN

Department of Marine, Earth and Atmospheric Sciences, North Carolina State University, Raleigh, NC 27695-8208, U.S.A.

(*First received* 6 *March* 1993 *and in final form* 8 *May* 1994)

Abstract—A soil–vegetation module is incorporated into a two-dimensional mesoscale model for simulating mesoscale circulations that develop due to changes in surface characteristics. The model was verified by evaluating the diurnal changes of heat fluxes, surface temperature, soil moisture and soil water content with different vegetation covers using a one-dimensional version. Thermally induced mesoscale circulations between vegetated and bare soil areas are simulated with the two-dimensional model using three different types of bare soil adjacent to the vegetated area. The properties of the vegetation breeze, which are similar to that of a sea breeze, are investigated. The intensity of the vegetation breeze circulation is directly related to the characteristics of the bare soil. There is a strong relationship between surface fluxes and the intensity of the vegetation breeze circulation. More soil moisture is transferred to the atmosphere over the vegetated area than over the bare soil area.

The effect of vegetation on planetary boundary layer (PBL) structure is presented by comparing the differences of turbulent kinetic energy (TKE), eddy diffusivity and boundary layer height between vegetated area and bare soil area. The effect of bare soil properties on PBL structure is also described.

Key word index: Vegetation forcing, surface energy budget, soil moisture, mesoscale circulation, boundary layer.

1. INTRODUCTION

Surface inhomogeneities, including boundaries between different types of vegetation and land use patterns, have important effects on the structure of the atmospheric boundary layer. Changes in the surface roughness, temperature and wetness make the planetary boundary layer (PBL) inhomogenous and produce substantial horizontal gradients of boundary layer characteristics (i.e. surface heat fluxes, turbulence, wind *et al.*). Significant differences in the surface thermal energy induce mesoscale circulations. Differences in soil moisture and vegetation cover have the most influence on the surface energy balance. Differential heating associated with variations in soil moisture can produce sea breeze type circulations (Ookuchi *et al.*, 1984). The generation of thermally induced flow by vegetated areas adjacent to bare soil areas has been investigated with different vegetation schemes (Mahfouf *et al.*, 1987; Segal *et al.*, 1988), by reducing the thermal gradients and therefore the strength of the induced circulations. Vegetation can modify sea breezes or daytime thermally induced upslope flows (Mahfouf *et al.*, 1987; Segal *et al.*, 1988). Micrometeorological observations from the HAPEX-MOBILHY field experiment (Pinty *et al.*, 1989) show that the atmosphere responds to discontinuities in vegetation type and soil moisture. The observation and two-dimension modeling studies show that significant circulations result at the interface between vegetation types or soil moisture amounts.

It is necessary to include the effect of vegetation in order to achieve a realistic simulation of low-level atmospheric properties and the planetary boundary layer structure and to realistically represent land surface processes. Pielke *et al.* (1991) used spectral analysis to demonstrate that there is a nonlinear influence of mesoscale landscape spatial variability on the atmosphere. The domain-averaged resolvable scale flux is sensitive to the averaging process when two vegetation cover types are included due to asymmetry in the thermally forced mesoscale circulation. The impact of changes in lower-boundary forcing through horizontal variations in soil and plant type has been reported by Modica *et al.* (1992). Their results showed that the use of a 1^0 resolution database of soil and vegetation type produced higher variances in simulated fields at most wavelengths when compared to simulations with a uniform distribution. Furthermore, the use of databases generated by random specification of soil and vegetation types resulted in higher variance at most wavelengths. The effect of

AE 29-16-5

the lateral boundary conditions was generally much greater in terms of the spectral magnitudes than that due to the soil–vegetation databases.

More comprehensive treatment of radiative and momentum surface transfers and surface hydrological parameterization are possible when vegetation is included in the simulation. Parameterization of the soil–vegetation–atmosphere system is required to capture subtle, interactions between these three systems. Deardorff (1978) developed a single-level canopy formulation containing many parameters with which to evaluate fluxes from the soil beneath the canopy as well as from the foliage itself. This model can be used with a nonisothermal surface for obtaining more realistic expressions of the vertical fluxes from the ground foliage system to the atmosphere compared to an isothermal canopy model (Noilhan and Planton, 1989). Single-layer canopy models are most appropriate for use in mesoscale and general circulation models (Raupach and Finnigan, 1988).

The objective of the present study is to incorporate Deardorff's vegetation scheme into a mesoscale model, which has turbulent kinetic energy closure and explicit cloud physics, to simulate the mesoscale circulation between a vegetated area and a bare soil area, and to investigate the PBL structure in the induced circulation with different bare soil types. In this paper we: (1) outline the main features of the mesoscale model and vegetation scheme, (2) present the results from the one-dimensional sensitivity experiments to examine the general behavior of the model with vegetation and the effect of variation in the vegetation cover, (3) investigate the characteristics of the induced mesoscale circulation associated with the so-called vegetation breeze using different bare soil types, vegetation stress transpiration condition and roughness length, (4) study the structure of turbulence and other PBL processes in the vegetation breeze and (5) analyze the feedback between surface heat fluxes and the vegetation breeze.

2. MODEL DESCRIPTIONS

2.1. *The mesoscale model*

The mesoscale model used here has been described by Huang and Raman (1991a, b). This model has been used in several numerical experiments (Huang and Raman, 1991a, b, 1992; Boybeyi and Raman, 1992) to establish its validity with different meteorological conditions and topographic features. The model is hydrostatic and anelastic in a terrain-following coordinate system. A five category cloud physics parameterization (Rutledge and Hobbs, 1983; Lin *et al.*, 1983) has been included. An upstream spline interpolation scheme is used for horizontal advection with a quadratic upstream interpolation in the vertical. The turbulence closure scheme is based on two prognostic equations, one for the turbulent kinetic energy (TKE) and the other for turbulent energy dissipation. The level 2.5 formulation of Mellor and Yamada (1982) is used to determine eddy diffusivity. Vertical diffusion terms are computed by a time-implicit scheme that allows the model to use a time step that is not constrained by turbulent diffusion. The mesoscale model is initialized based on a 1-D PBL model solving the Ekman-gradient wind equations for the flow over the ground. Orlanski's radiation condition (Orlanski, 1976) with forward-upstream scheme (Miller and Thorpe, 1981) is used at the lateral boundaries. To minimize the thermal gradients that can be generated due to the imposed boundary conditions, a first-order upstream scheme is applied at grids closest to the lateral boundaries. A radiation boundary condition (Klemp and Durran, 1983) is used at the upper boundary to determine the perturbation pressure at the top level of the domain. This radiation condition allows outward propagation of wave energy.

2.2. *The vegetation scheme*

The vegetation scheme follows that developed by Deardorff (1978). The scheme provides for heat and water exchanges at the land surface. It includes a representation of a single vegetation layer and two soil layers. Evapotranspiration is determined as if the plant canopy were not more than a partly wet plane at the lower boundary of atmosphere. Plant evapotranspiration can be expressed in terms of measurable weather parameters together with the physiological and aerodynamic resistance. Plant transpiration requires energy to supply the latent heat of conversion of water from the liquid to the vapor phase, and also involves diffusion of water vapor away from the transpirating surface. A bulk stomatal resistance for diffusion from the evaporating sites within the leaf-to-leaf surface and a bulk aerodynamic resistance for diffusion from the surface to the well-mixed surrounding air are included. The saturation deficit is used to calculate evaporation or condensation from or onto the leaf. Condensation which occurs on the soil surface is not treated as dew but is simply added to the bulk soil moisture budget. The ground surface temperature and soil moisture are obtained by solving simultaneously the energy budget and water budget equations at the soil–vegetation–air interface, respectively. The prognostic equations for the soil temperature and soil water content are described below. The ground surface temperature T_g is calculated by "force-restore" method:

$$\frac{\partial T_g}{\partial t} = -c_1 \frac{H_A}{\rho_s c_s d_1} - c_2 \frac{T_g - T_2}{\tau_1} \tag{1}$$

where H_A is the ground surface energy, d_1 is a soil depth influenced by the diurnal temperature cycle, c_1, c_2 are constants, τ_1 is a diurnal period, ρ_s is the soil density, c_s is the soil thermal heat capacity. The mean deep soil temperature T_2 is

$$\frac{\partial T_2}{\partial t} = -\frac{H_A}{\rho_s c_s d_2} \tag{2}$$

where d_2 is a soil depth influenced by seasonal moisture variations. The moisture budget equation that describes the vertical diffusion processes for the ground surface and the root layer is

$$\frac{\partial w_g}{\partial t} = -C_1 \frac{E_g + 0.1E_{tr} - P_g}{\rho_w d_1'} - C_2 \frac{w_g - w_d}{\tau_1} \quad (3)$$

where w_g is volumetric concentration of soil moisture at the ground surface, w_d is soil moisture content within the root layer, ρ_w is density of water, E_g is evaporation rate at the ground surface, E_{tr} is foliage transpiration rate, C_1, C_2 are coefficients and d_1 is a soil depth (10 cm) influenced by the diurnal soil moisture cycle. The time-dependent equation for w_d is

$$\frac{\partial w_d}{\partial t} = -\frac{E_g + E_{tr} - P_g}{\rho_w d_2'} \quad (4)$$

where P_g is the precipitation rate at ground level and d_2' is a soil depth (50 cm) influenced by seasonal moisture variations. The conservation equation for mass of liquid water retained by foliage is given by

$$\frac{\partial w_{dew}}{\partial t} = \sigma_f P - (E_f - E_{tr}) \quad 0 \leqslant w_{dew} \leqslant w_{dmax} \quad (5)$$

where w_{dew} is mass of liquid water retained by foliage per unit horizontal ground area, w_{dmax} is maximum value of w_{dew} beyond which runoff to soil occurs, σ_f is foliage shielding factor of ground from shortwave radiation, E_f is evaporation rate in foliage surface and P is precipitation rate.

3. THE NUMERICAL RESULTS

3.1 1D *sensitivity experiments*

One-dimensional simulations were used to examine the general behavior of the model with vegetation. Two different sets of sensitivity experiments were performed to investigate the diurnal effect of vegetation on surface heat fluxes, temperature and moisture, and to investigate the influence of variation in the vegetation cover onto atmosphere and soil hydrology. The first of sensitivity experiments were 10 day runs in which a constant foliage shielding factor (σ_f) of 0.75 was assumed. Precipitation was prescribed in this simulation to examine the response of the surface variables and soil moisture. In the second simulation, the foliage shielding factor was varied from 0.1 to 1.00 for 3 days. In all one-dimensional experiments, the constants and initial conditions were taken from Deardorff's original data set. Soil moisture in the below-surface layer in both cases was set to close to the saturated value. The ground surface temperature was modified for mid-latitude in the early summer (283 K). The initial atmospheric conditions are stable. The beginning of simulation was at 0500 local time.

The foliage or leaf surface temperature (T_f), the mean air temperature within a canopy (T_{af}) and the ground surface temperature (T_g) are shown in Fig. 1a, demonstrating the effect of vegetation. The foliage temperature (Fig. 1a) is significantly larger (4 K) than the ground surface temperature during midday. Foliage temperature is also larger than the surrounding air temperature, producing a stable surface condition. The diurnal variation of foliage surface moisture (q_f), the mean specific humidity of air within the canopy (q_{af}), and the mean specific humidity at ground surface (q) are shown in the Fig. 1b. The foliage moisture becomes less than ground surface moisture at night, promoting condensation onto the foliage. Foliage moisture exceeds surface moisture during the early morning hours but as the strong daytime solar radiation evaporates the moisture, the foliage moisture becomes less than the surface moisture in the afternoon. The simulated diurnal cycle for both temperature and moisture regulates the corresponding heat fluxes and indicates the importance of foliage cover on the atmospheric energy balance. A small amount of precipitation (1 mm h^{-1}) is prescribed in the one-dimensional model simulation between 120 and 130 h. The results show the sensitivity to this change. The diurnal maximum values of temperature decrease and the moisture increases during precipitation. The temperature and moisture values return to the steady-state value after about 24 h.

A foliage shielding factor (σ_f) of 0.1 corresponds to very little vegetation and a value of 1.0 corresponds to complete vegetation cover. The diurnal variation of ground temperature for different foliage shielding factors are shown in Fig. 2a. For dense vegetation cover, the ground temperature is lower than that for the case with sparse vegetation cover. A significant temperature difference (14 K) exists between the two extreme vegetation covers. The temperature difference is larger during daytime and much less during nighttime. The maximum difference during the early afternoon is consistent with the heat capacity of dense vegetation. Changes in the ground surface moisture for different shielding factors also show the importance of vegetation (Fig. 2b). With dense vegetation, moisture near the surface is smaller than with a sparse vegetation cover because there is less evapotranspiration and less leaf interception in the latter case. However, there may be more evaporation from a soil surface with sparse vegetation cover. Evapotranspiration is negligible at night; therefore, ground surface moisture is independent of the vegetation cover, and the moisture differences are small for different values of σ_f at night.

Energy fluxes at a land surface including vegetation are calculated from the underlying ground and the foliage above. The partitioning of available energy between the sensible and latent heat fluxes is sensitive to the land surface characteristics. The sensible heat flux depends on the temperature differences between ground surface and foliage air temperature as well as between the leaf surface and above leaf air temperatures. Energy storage in the vegetation layer is ignored. The latent heat flux is related to the wetness of

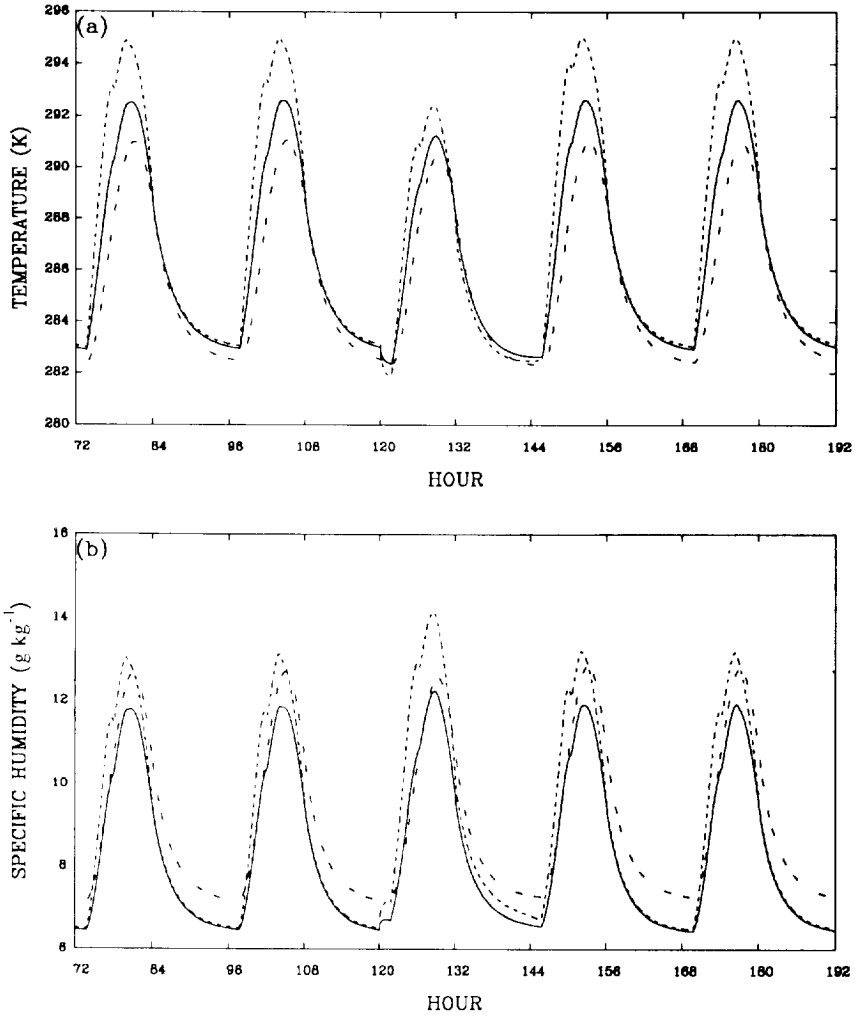

Fig. 1. The diurnal cycle of (a) temperatures (K) and (b) specific humidities (g kg^{-1}) for hours 72 to 192 from a 10 day simulation. Precipitation is prescribed between 120 and 130 h. The solid lines represent the values within canopy (T_{af} and q_{af}), the dashed lines represent foliage values (T_f and q_f) and the long dashed lines represent ground surface values (T_g and q_g).

the surface, evaporation from the ground and transpiration from the foliage. Sensible heat flux dominates and the Bowen ratio is greater than 1 during daytime (Fig. 3). At night, the surface temperature cools sufficiently to allow the surface humidity to fall below the humidity in the air. The flux of water vapor onto the surface may result in condensation at the surface. And the Bowen ratio becomes less than 1. The negative sign of Bowen ratios indicates that the change of sensible and latent heat flux is not in phase near sunset. After the precipitation from hour 120 to hour 130, latent heat flux dominates during daytime with more condensation at night as large amounts of atmospheric moisture produces latent heat flux from air to the ground surface.

The volumetric moisture content in the soil surface (w_g) and in the root layer (w_d) are shown in Fig. 4 to quantify the response of soil moisture to atmospheric forcing. Soil moisture is a source of evaporation of water. Sufficient soil moisture in the root layer can transpire more moisture into atmosphere through the stomata of vegetation. Vaporization of water takes place from the soil surface layer. With less vegetation cover, more daytime evaporation and nighttime condensation at the surface leads to a larger diurnal change in soil surface moisture (w_g) (Fig. 4a). Because of more evaporation than condensation for small foliage shielding factor, soil surface moisture also decreases with time. With a dense vegetation cover, the evaporation from the surface layer to the atmosphere is less important than transpiration from the root layer to atmosphere. Therefore, soil surface moisture has little diurnal change. Cooler temperatures at ground surface (day or night, compared to foliage temperature, see Fig. 1) allow the flux of water vapor into the surface, and moisture flux is transferred

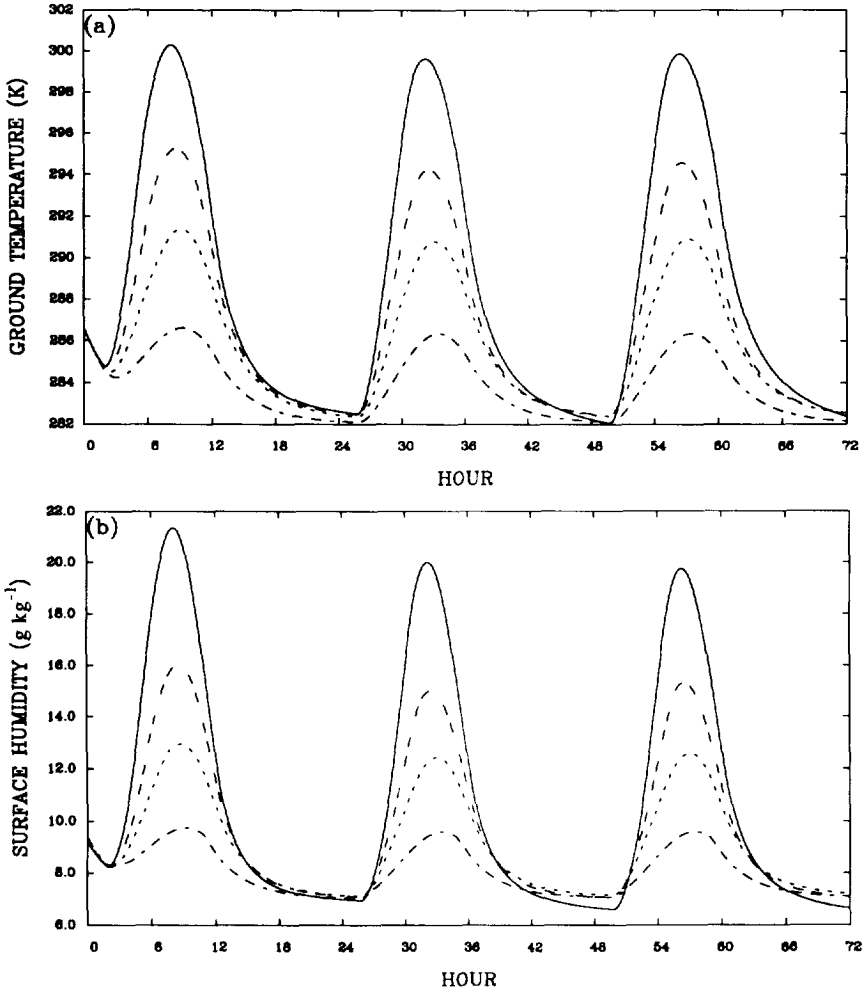

Fig. 2. The diurnal cycle of (a) the ground surface temperature (K) and (b) specific humidity ($g\,kg^{-1}$) as a function of leaf shielding fraction, which varied from 0.1 (solid line), 0.5 (long dashed line), 0.75 (dashed line) to 1.00 (alternating dashed dot line).

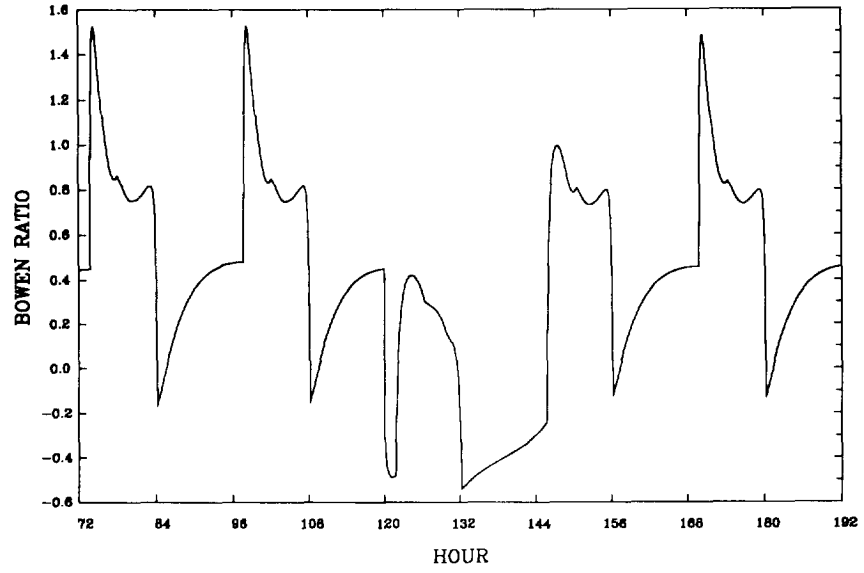

Fig. 3. The Bowen ratio for hours 72 to 192 from a 10 day simulation. Precipitation is prescribed between 120 and 130 h.

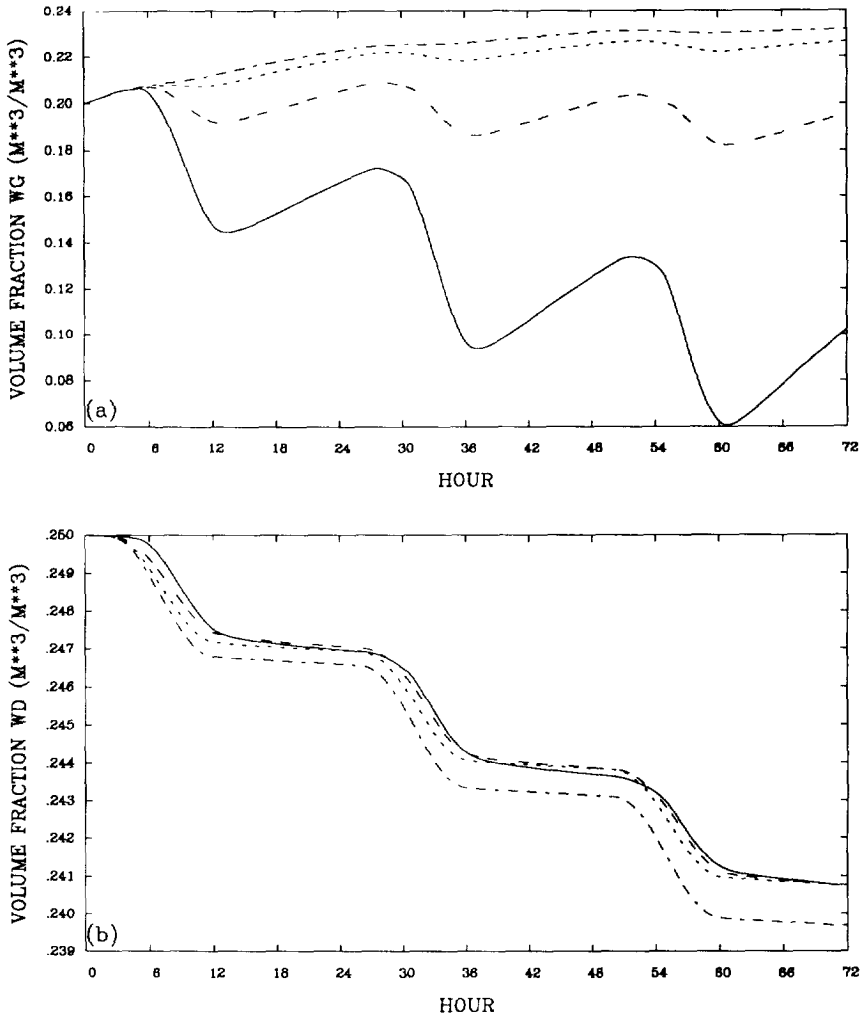

Fig. 4. The volumetric moisture content of (a) the soil surface layer ($m^3 m^{-3}$) and (b) the deeper root zone ($m^3 m^{-3}$) as a function of leaf shielding fractions. The dashed line scheme is the same as in Fig. 2.

from the root layer by diffusion, so the amount of soil surface moisture increases slightly. Figure 4b shows the root layer volumetric moisture change with time. There is a decrease during daytime due to transpiration, which increases with the vegetation cover. There is no transpiration during night, so the amount of moisture in the root zone remains constant. Due to greater transpiration, the moisture in the root layer is depleted more rapidly for dense vegetation cover.

3.2. *2D simulations*

Two-dimensional experiments were designed to investigate the effect of different bare soil types on inducing mesoscale circulations between the vegetated area and the bare soil area. Three cases with different bare soil types (clay, loam and sand) are presented. The different vegetation and soil parameters used for the three experiments are shown in Table 1. The initial atmospheric conditions of all three experiments are identical. The initial surface temperature is 300 K with a potential temperature lapse rate of $+3.5\ K\ km^{-1}$. The initial wind field is $-1.0\ m\ s^{-1}$. The model domain is 1200 km × 7 km in the horizontal and vertical, with higher resolution in lower levels and a uniform horizontal grid length of 5 km. The time step is 20 s. The starting time of the experiments is 0800 local time for mid-summer conditions. The astronomical parameters for solar radiation correspond to 15 August at a latitude of 32°N.

3.2.1. *Vegetation breeze and mesoscale circulations.* Mesoscale circulations develop over the interface between the vegetated area and the bare soil area because of the heterogeneity of surface characteristics and thermal flux differences. Near the surface, the wind flows from the vegetated area to the bare soil (Fig. 5a), the so-called vegetation breeze (Tjernström,

Table 1. Vegetation and soil characteristics for three experiments

	Unit	Value
Vegetation type		
Canopy albedo		0.2
Canopy emissivity		0.95
Roughness length	m	0.5
Minimum stomatal resistance	$s\,m^{-1}$	200
Leaf shielding factor		0.9
Depth of surface	m	0.1
Depth of root layer soil moisture	m	0.5
Initial surface soil moisture	$m^3\,m^{-3}$	0.25
Initial root layer soil moisture	$m^3\,m^{-3}$	0.25
Soil type		
Soil emissivity		1.00
Soil albedo		0.25
Roughness length	m	0.02
Initial surface soil moisture	$m^3\,m^{-3}$	0.05
Initial root layer soil moisture	$m^3\,m^{-3}$	0.05
Soil thermal diffusivity	$\times 10^{-4}\,m^2\,s^{-1}$	
Clay		0.012
Loam		0.0015
Sand		0.002
Dry volumetric heat capacity	$\times 10^6\,Jm^{-3}\,K^{-1}$	
Clay		1.2558
Loam		4.186
Sand		2.3

1988). In this figure and subsequent figures representing vertical cross sections, results from interior 300 km and lowest 3.5 km of the domain are presented. The mesoscale circulation associated with a vegetation breeze has characteristics similar to a seabreeze except that the magnitude and onset time may be different. The mechanism of the vegetation breeze is similar to the daytime sea breeze studied by Sun (1981a, b). Mass is mixed upward over the bare soil by greater turbulent mixing in the unstably stratified boundary layer, creating a pressure gradient from the bare soil area to the vegetated area at some distance above the ground. The resultant flow from bare soil to the vegetated area above the ground near the interface creates a low-pressure region at the ground, and the vegetation breeze develops (Pielke, 1984). Upward motion occurs over the bare soil area and downward motion occurs over the vegetated area (Fig. 5b) with weaker downward motion over the bare soil away from the interface. This compensating downdraft over the bare soil is consistent with results given by Smith and Lin (1982), and Lin and Smith (1986). They used linear perturbation theory to investigate the response of a stratified atmosphere to a local heat source. An updraft at the center of a steady-state heat source is surrounded by compensating downdrafts. In the present study, the local heating is referred to as the heating disturbance at the interface between the vegetated area and the bare soil area (Fig. 5c).

Most of the following discussion in this section is for loam soil. The results for all three cases are summarized in Fig. 6, which shows the time evolution of the maximum and minimum wind speed. To highlight the induced circulation, the u component of the wind has the initial $-1.0\,m\,s^{-1}$ wind subtracted. The general characteristics for the three cases are consistent. The strongest wind speeds occur with sandy soil, which has the smallest heat capacity and the weakest wind speeds occur with clay which has the greatest heat capacity.

Loam has soil heat capacity greater than sand but smaller than clay. The intensity of the circulation that developed was less than that for sand, and greater than that for clay. The onset time for the vegetation breeze is about 3 h into the simulation with loam soil. The maximum u component reaches $3.9\,m\,s^{-1}$ at hour 6 and $5.8\,m\,s^{-1}$ at hour 9. The values of wind speed in the late afternoon are relatively small compared to other model results (Segal *et al.*, 1988). This is because of lower sensible heat flux by different heat capacity for both vegetation and bare soil. The vertical velocities are consistent with the horizontal velocities with maximum values where the horizontal convergence is greatest. The maximum vertical velocity is $11.4\,cm\,s^{-1}$ after 6 hours and $21.1\,cm\,s^{-1}$ after 9 hours. The wind speed increases with time because the balance between the production term associated with horizontal pressure gradient force and the dissipation term associated with the turbulent mixing is broken by decreasing turbulent mixing.

This thermal induced circulation, under favorable large-scale atmospheric conditions, may be involved with the triggering and development of local convective clouds, which may result in increased convective precipitation. The interaction between the induced mesoscale circulation, atmospheric water vapor and

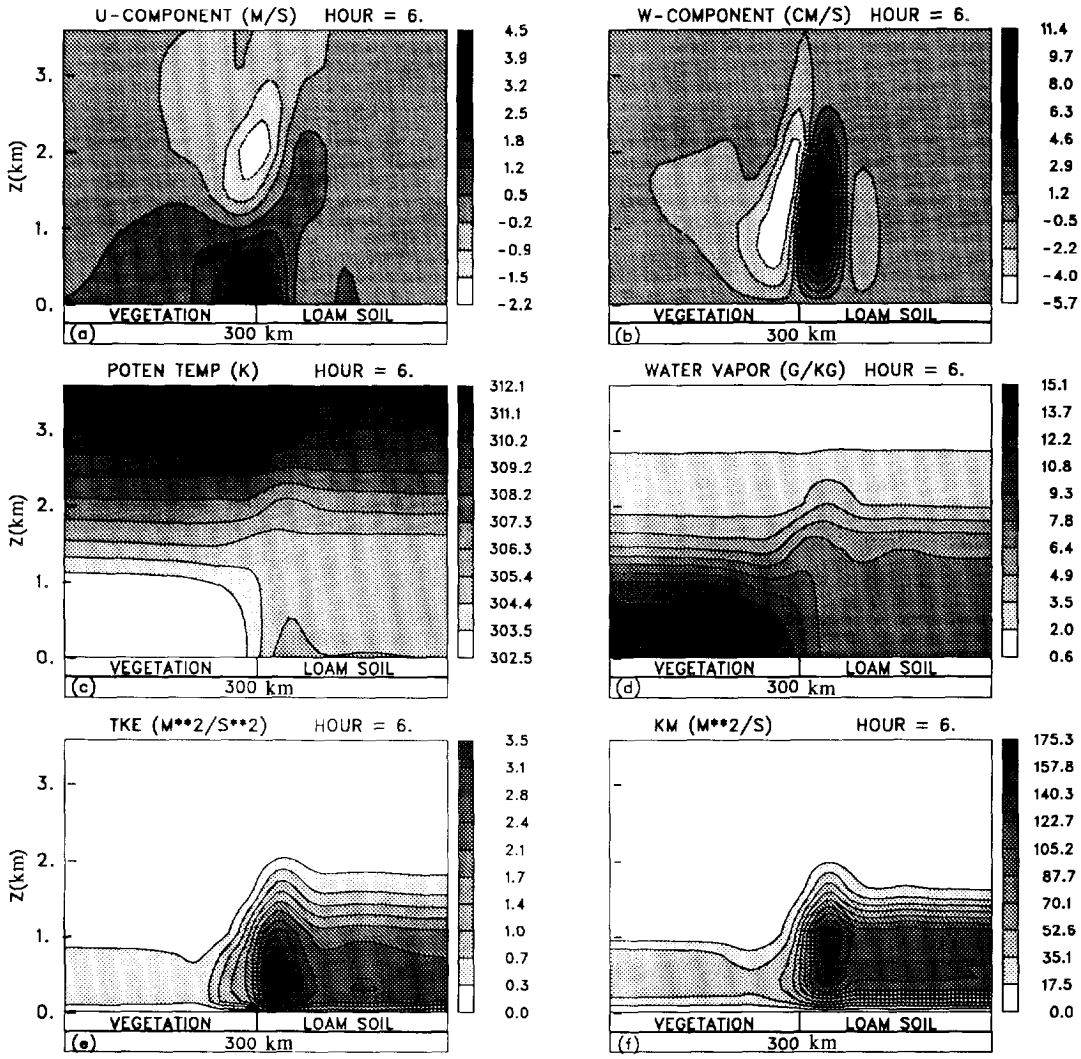

Fig. 5. The vertical cross section of (a) horizontal wind speed ($m\,s^{-1}$), (b) vertical wind speed, (c) potential temperature (K), (d) water vapor ($g\,kg^{-1}$), (e) turbulence kinetic energy ($m^2\,s^{-2}$) and (f) momentum eddy diffusivity ($m^{-2}\,s^{-1}$) 6 h into a simulation with loam bare soil adjacent to a vegetated area. The results are presented for the lower 3.5 km and the horizontal extent is 300 km. The gray scale bar on the right indicates the range and shading values for the variables.

convective precipitation has been supported observationally and theoretically (Anthes, 1984). There is more water vapor over the vegetated area through most of the boundary layer than over the bare soil area as vegetation exerts physiological control upon the transpiration rate (Fig. 5d). The water vapor in the lower boundary layer over vegetated area is about two times larger than that over bare soil area. High soil moisture content is prescribed in the vegetated area initially to provide a nonstressed transpiration condition. There is larger latent heat flux over the vegetated area than over the bare soil area as the vegetation efficiently pumps moisture into the atmosphere from the root zone (Fig. 7). The amount of latent heat flux for 6 h simulation is 255 $W\,m^{-2}$ over the vegetated area and 82 $W\,m^{-2}$ over bare soil area. The partitioning of energy at the surface depends on the wetness of the surface, and on the amount of moisture in the soil near the surface. Initial dry bare soil conditions lead to the smaller values of latent heat flux.

Baroclinicity is created in the boundary layer due to larger sensible heat flux over the bare soil (Fig. 5c). More absorbed radiative flux is partitioned into sensible heat flux, as latent heat flux is small. The differential heating throughout the boundary layer creates the horizontal gradient of pressure, which then generates vegetation breeze at the interface between the bare soil and the vegetated area with return flow at the top of the boundary layer (Fig. 5a).

The turbulence characteristics include the turbulent kinetic energy (TKE), the viscous dissipation rate (ε) of TKE, and eddy diffusivity for momentum (K_M) as well

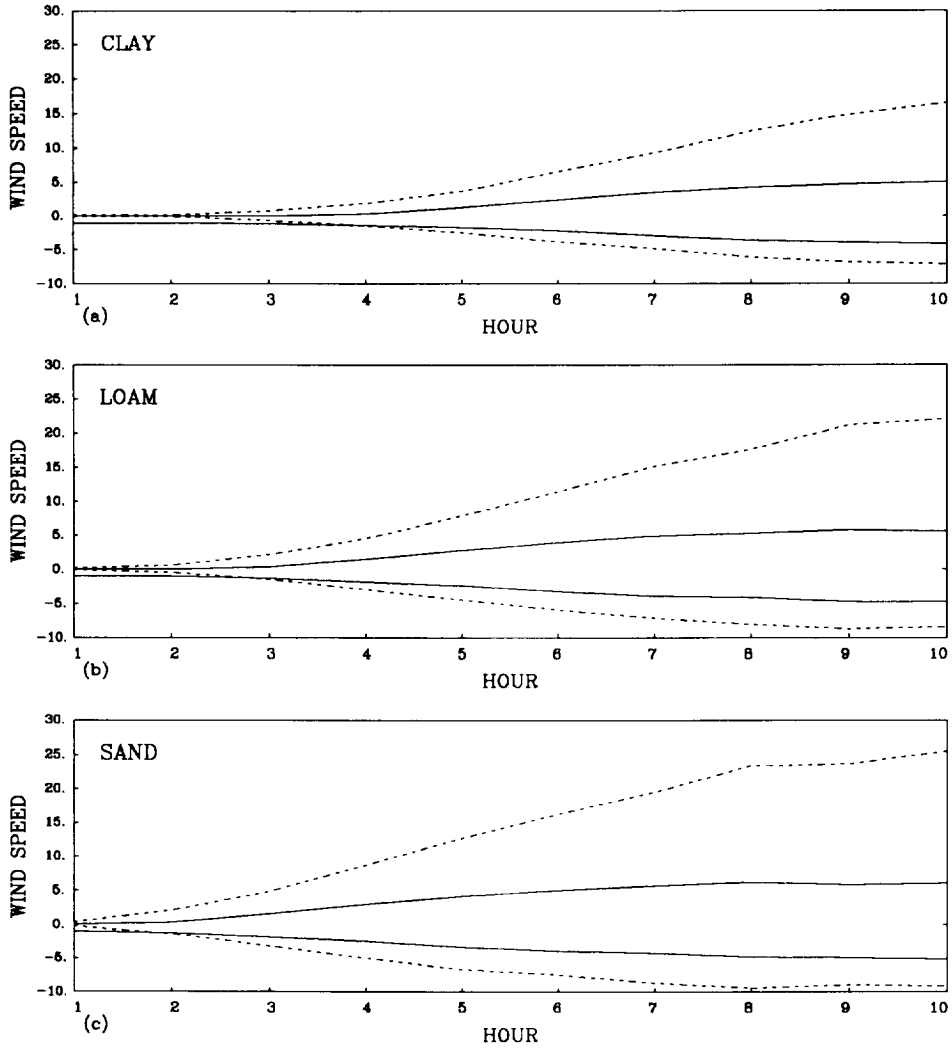

Fig. 6. The time evolution of maximum and minimum wind speed for (a) clay, (b) loam and (c) sand. The solid lines represent horizontal wind speed ($m\,s^{-1}$) and the dashed lines represent vertical wind speed ($cm\,s^{-1}$).

as for heat (K_H). Vegetation affects turbulence through friction (roughness) and thermal transport. Many observations of turbulent exchange between a forest and the atmosphere have been reported (Hutchison and Hicks, 1985). The maximum turbulence appears at the interface where the vegetation breeze originates. Greater buoyancy production over the bare soil leads to greater TKE, which in turn leads to greater mixing throughout the boundary layer (Fig. 5e). The maximum TKE values increase as the induced mesoscale circulations develop. The viscous dissipation is the sink for TKE. Its variation is similar to that of TKE, and its magnitude increases with time. Since eddy diffusivity is parameterized by the mixing length and TKE, the structure of the eddy diffusivity is also similar to that of the TKE (Fig. 5f). The eddy diffusivity for momentum (K_M) is used to emphasize the variations in the PBL.

3.2.2. *Vegetation breeze circulations and bare soil heat capacity.* Differential soil heat capacity creates differences in the sensible heat flux from the ground to the atmosphere. Results of three numerical experiments designed to investigate the effect of different soil types in inducing mesoscale circulations between the vegetated area and the bare soil area are presented in this section. Different parameters used for the three soil types are shown in Table 1. The vegetation characteristics are the same for all three cases.

The time evolution of surface heat fluxes for the three cases can be found in Fig. 7. All the three soil types produce stronger sensible heat fluxes over the bare soil area with larger latent heat flux over the vegetated area. The clay surface has the largest heat capacity compared to other two soil types and thus there is less sensible heat flux to atmosphere. The sandy surface, which has the smallest heat capacity,

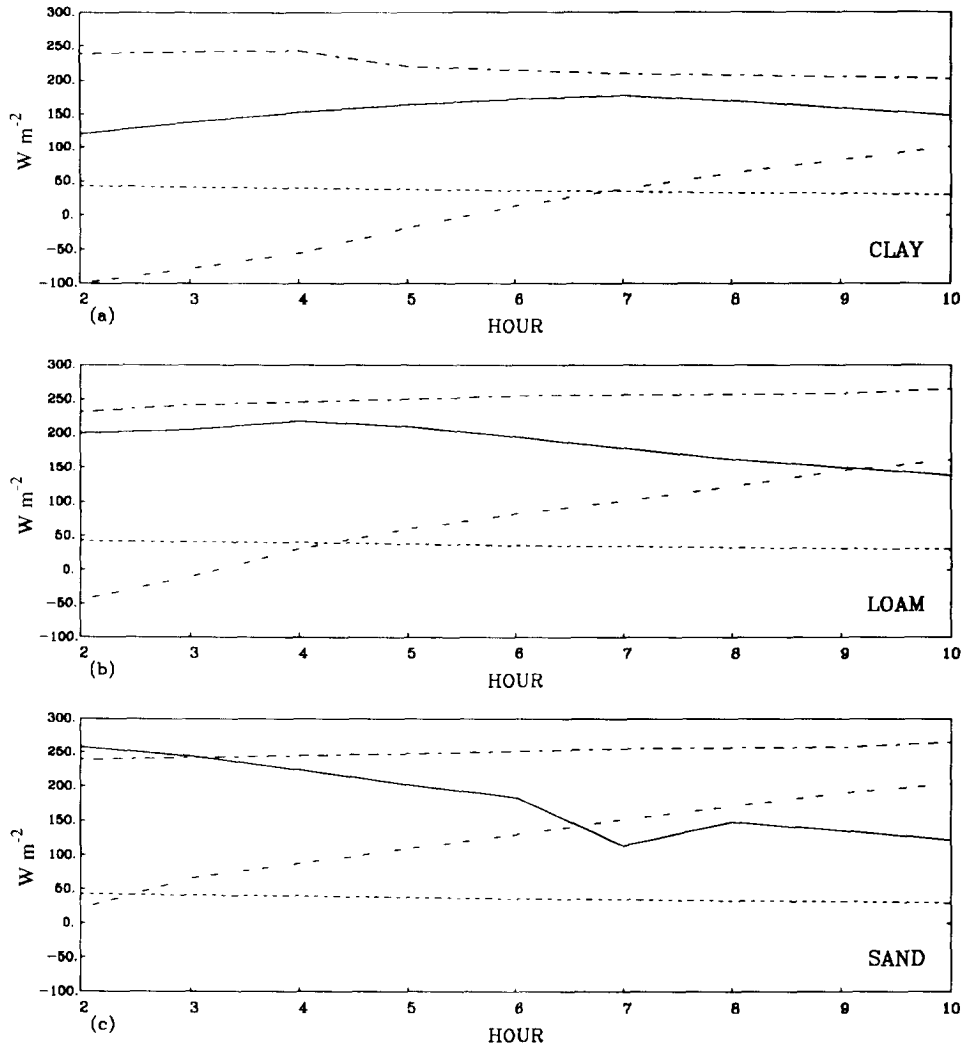

Fig. 7. The time evolution of sensible and latent heat fluxes for (a) clay, (b) loam and (c) sand. The solid line and long dashed line represent sensible and latent heat fluxes over bare soil areas respectively. The short dashed line and alternating dashed dot line represent sensible and latent heat fluxes over vegetated areas respectively.

transfers the most sensible heat flux producing the strongest horizontal gradients between bare soil and vegetated area.

The results show that the partitioning of surface heat fluxes that regulates feedback to the atmosphere from bare soil is strongly related to surface characteristics. Sensible heat flux dominates over bare soil area and is sensitive to soil heat capacity. Differential soil heat capacity creates differences in the sensible heat fluxes. There is 1.8 times more sensible heat flux for sandy soil than for clay at hour 3. Larger values of sensible heat flux provided more direct heating of the lower atmosphere, resulting in a larger horizontal pressure gradient and a more rapid development of a mesoscale circulation. This is demonstrated by the results of the cross section of horizontal and vertical velocities at hour 3 (Fig. 8). The vertical velocities for the sandy case are two times greater than those for loam and are six times greater than those for clay. The circulation strength is also apparent in the horizontal velocity, although not as dramatic. There is low level acceleration at the interface and a return flow at the top of the PBL has started to develop in all cases. The circulation is strongest for sandy soil and weakest for clay. The relative strength of the circulation is evident by examining the horizontal and vertical velocities for sand and clay (Fig. 9). The compensating downdraft is stronger for sandy soil case as heating at the interface between the vegetated area and bare soil area is greatest.

Feedback to the surface heat fluxes induced by the vegetation breeze circulation also can be seen in Fig. 7. The sensible heat flux increases at the beginning and eventually decreases with time in all three cases. The

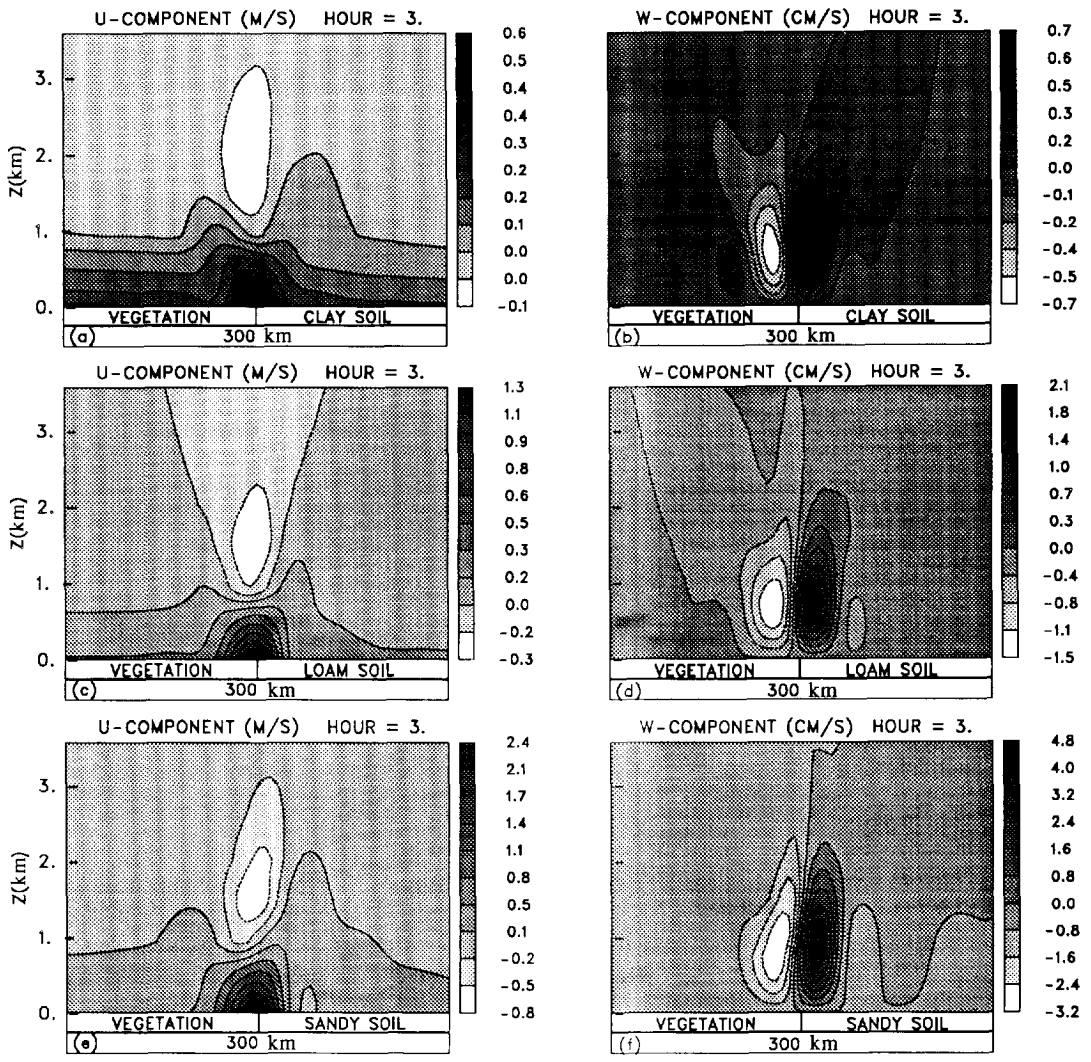

Fig. 8. The horizontal and vertical wind components from simulations at hour 3 with bare soil to clay (a, b), loam (c, d) and sand (e, f) for the same domain as in Fig. 5. The gray scale bar on the right indicates the range and shading values for the variables.

decrease of the sensible heat flux is more rapid for sand than for clay which has a higher soil heat capacity. The sensible heat flux is larger for clay than for sand after hour 7 while latent heat flux continues to increase. That is consistent with sea breeze characteristics. After the circulation is well developed, the vegetation breeze transfers cool moist air from the vegetated area to the bare soil area. Changed temperature and water vapor again determine the partitioning of sensible and latent subgrid scale fluxes over the bare soil. Sandy soil is more sensitive to this feedback because a more intense circulation is generated. This result is consistent with that studied by Mahfouf *et al.* (1987). He indicated that vegetation in a dry environment modifies the surface fluxes in a significant way. Its role here is to reduce the large difference between sensible and latent heat fluxes existing over bare soil by decreasing the sensible heat as the evapotranspiration increases. The reduction in this difference tends to reduce the induced mesoscale circulation.

The maximum PBL height from the TKE to determine the effect of vegetation on PBL corresponding to the mesoscale circulation can be inferred in Fig. 10. The greatest values of TKE appear with sandy soil due to large buoyancy production. The smallest TKE values are with clay, where sensible heat flux and buoyancy production are minimum. The generation of TKE through buoyancy production induces the mesoscale circulation. The circulation develops earliest and strongest over sand, latest and weakest over clay. The height of the boundary layer is greatest over the bare soil and grows to approximately the same height for all three soil types. The intensity of TKE is greatest for sand and weakest for clay, related to the amount of

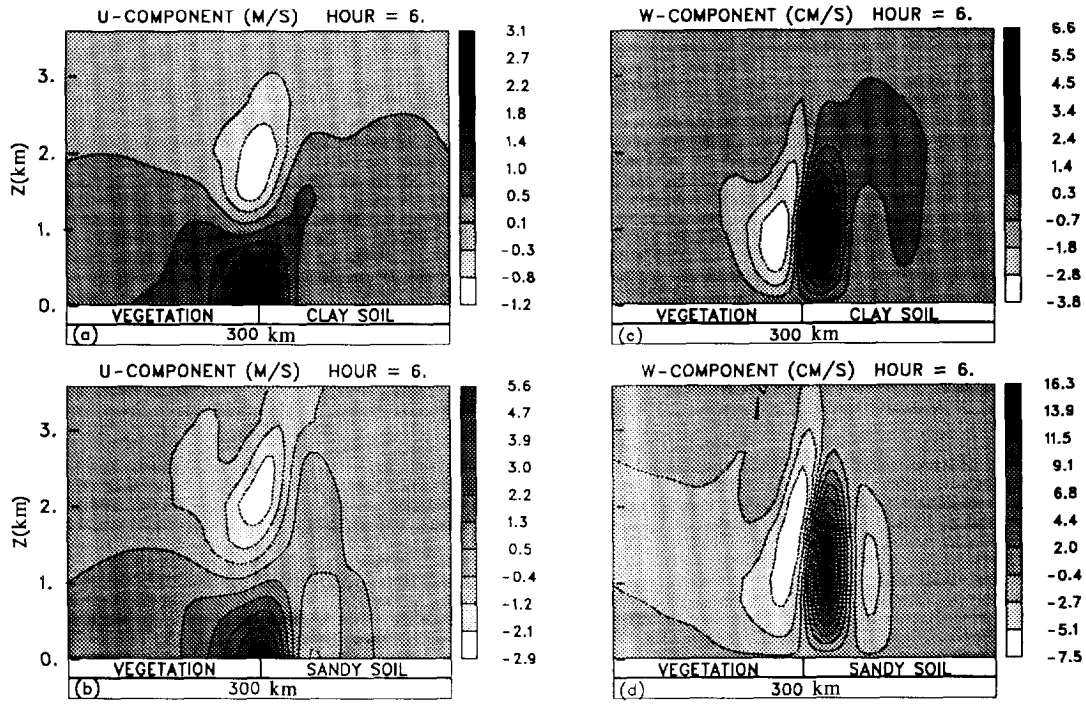

Fig. 9. The horizontal and vertical wind components for clay (a, b) and sand (c, d) from simulations at hour 6 with the same domain as presented in Fig. 5. The gray scale bar on the right indicates the range and shading values for the variables.

sensible heat flux. At hour 3, TKE is greater over the vegetated area for clay and loam. However, over sand with a smaller heat capacity, the surface heat flux has generated larger TKE than over the vegetated area. This explains the earlier onset of the mesoscale circulation over sand. The higher values of TKE that persist over sand through nine hours explains the maintenance of the stronger circulation.

4. CONCLUSIONS

This paper demonstrates that the role of vegetation in generating mesoscale circulation is significant by incorporating a soil–vegetation module into a two-dimensional mesoscale model.

A one-dimensional version of the model was evaluated by examining diurnal changes of heat fluxes, surface temperature, soil moisture and soil water contents with different vegetation covers. The results showed that the foliage temperature is significantly larger than the underlying ground surface temperature, which then produces a stable surface condition. A vegetation layer modifies moisture transfer into the atmosphere by evapotranspiration or condensation related to deep soil water content. Ground surface temperature is strongly dependent on the vegetation cover. There is a significant temperature difference between dense vegetation cover and sparse vegetation cover, but the ground surface moisture difference is relatively small. The modified temperature and moisture regulate the corresponding heat fluxes and change the atmospheric energy balance. The partitioning of available energy between sensible and latent heat fluxes is sensitive to land surface characteristics and also responds to precipitation.

The moisture content in the soil surface and in the root layer is related to vegetation cover. Soil surface moisture content has a larger diurnal change and dries out more rapidly when the surface has less vegetation cover. The soil moisture has a smaller diurnal change and increases slightly when the surface has a dense vegetation cover. Root layer soil moisture content also depends on vegetation cover. Stomatal transpiration of vegetation is an increasingly important effect as vegetation cover increases.

Thermally induced mesoscale circulation between vegetated and bare soil areas was generated by a two dimensional model with three different types of bare soil adjacent to a vegetated area. The properties of the vegetation breeze are similar to that of sea breeze. More soil moisture is transferred to the atmosphere over the vegetated area than over the bare soil area as the vegetation efficiently pumps moisture into the atmosphere from the root zone. Higher values of the sensible heat flux occur over the bare soil area as less energy is partitioned into latent heat flux. The intensity of the vegetation breeze circulation is strongly related to the characteristics of the bare soil. The vegetation breeze circulation is strongest when cou-

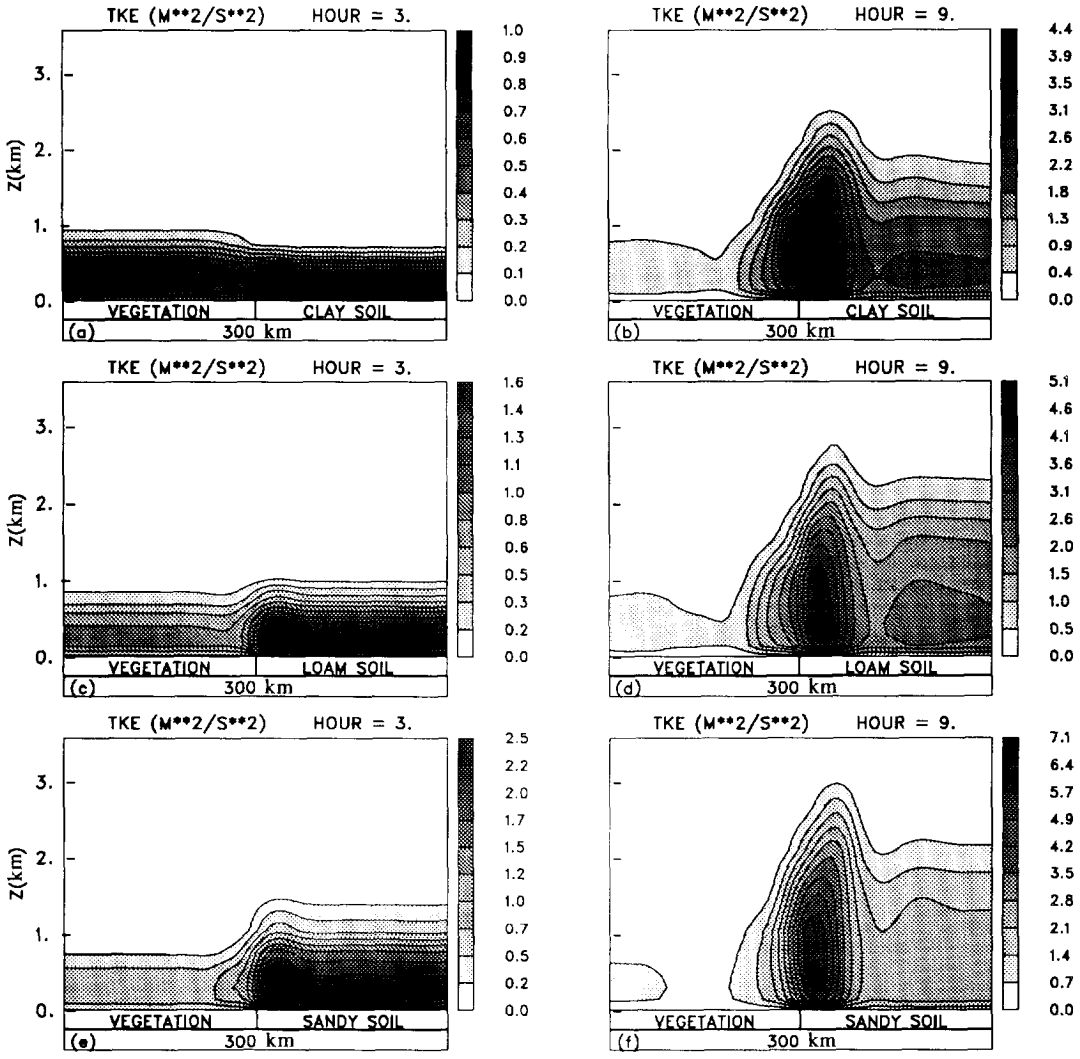

Fig. 10. Turbulence Kinetic Energy (TKE) from simulations at hour 3 and 9 for clay (a, b), loam (c, d) and sand (e, f) with the same domain as presented in Fig. 5. The gray scale bar on the right indicates the range and shading values for the variables.

pled with sandy bare soil and is weakest when coupled with clay. There is also a strong relationship between surface fluxes and the intensity of the vegetation breeze circulation. Surface heat flux gradients generate the circulation, which in turn reduces the horizontal gradient of heat fluxes. Sensible heat flux decreases and latent heat flux increases over bare soil as the vegetation breeze increases and transfers more moisture and cool air from the vegetated area to the bare soil area. A horizontal soil moisture gradient coupled with the thermally induced mesoscale circulation could alter the local weather and climate and affect the hydrologic cycle through soil water content.

The effect of vegetation on PBL structure is demonstrated by comparing the differences of TKE, eddy diffusivity and boundary layer height between vegetated area and bare soil area. The maximum turbulence appears near the interface where the vegetation breeze circulation is generated and increases as the circulation develops strongly. The changes of bare soil properties with the same vegetation type significantly affect the PBL structure. Turbulent mixing is greatest with sandy bare soil, which has the least soil heat capacity of the three soil types. The depth of the PBL appears to be independent of the soil type, but intensity of the mesoscale circulation depends on the amount of turbulent mixing and, therefore, on soil type.

Acknowledgements –This work is supported by the U.S. Department of Energy ARM program, under contract number 091575-A-Q1 with Pacific Northwest Laboratories. Computer time was provided by the DOE at the National Energy Research Supercomputer Center and by the North Carolina Supercomputing Center.

REFERENCES

Anthes R. (1984) Enhancement of convective precipitation by mesoscale variations in vegetative covering in semiarid regions. *J. Clim. Appl. Met.* **23,** 541–554.

Boybeyi Z. and Raman S. (1992) A three-dimensional numerical sensitivity study of convection over the Florida peninsula. *Boundary-Layer Met.* **60,** 325–359.

Deardorff J. W. (1978) Efficient prediction of ground surface temperature and moisture, with inclusion of a layer of vegetation, *J. geophys. Res.* **20,** 1889–1903.

Huang C.-Y. and Raman S. (1991a) Numerical simulation of January 28 cold air outbreak during GALE, part I: The model and sensitivity tests of turbulence closures. *Boundary-Layer Met.* **55,** 381–407.

Huang C.-Y. and Raman S. (1991b) Numerical simulation of January 28 cold air outbreak during GALE, part II: The mesoscale circulation and marine boundary layer. *Boundary-Layer Met.* **56,** 51–81.

Huang, C.-Y. and Raman S. (1992) A three-dimensional numerical investigation of a Carolina coastal front and the Gulf Stream rainband. *J. atmos. Sci.* **49,** 560–584.

Hutchison B. A. and Hicks B. B. (1985) *The Forest–Atmosphere Interaction.* Reidel, Dordrecht.

Klemp J. B. and Durran D. R. (1983) An upper boundary condition permitting internal gravity wave radiation in numerical mesoscale model. *Mon. Wea. Rev.* **111,** 430–444.

Lin Y.-L. and Smith R. B. (1986) Transient dynamics of airflow near a local heat source. *J. atmos. Sci.* **43,** 40–49.

Lin Y.-L., Farley R. D. and Orville H. D. (1983) Bulk parameterization of the snow field in a cloud model. *J. Clim. appl. Met.* **22,** 1065–1092.

Mahfouf J.-F., Richard E. and Mascart P. (1987) The influence of soil and vegetation on the development of mesoscale circulations. *J. Clim. appl. Met.* **26,** 1483–1495.

Mellor G. L. and Yamada T. (1982) Development of a turbulence closure model for geophysical fluid problems. *Rev. geophys. Space Phys.* **20,** 851–875.

Miller M. J. and Thorpe A. J. (1981) Radiation conditions for the lateral boundaries of limited area numerical models. *Q. J. R. met. Soc.* **107,** 615–628.

Modica G. D., Yee S. Y.-K. and Venuti J. (1992) Some effects of soil and vegetation databases on spectra of limited-area mesoscale simulations. *Mon. Wea. Rev.* **120,** 2067–2082.

Noilhan J. and Planton S. (1989) A simple parameterization of land surface processes for meteorological models. *Mon. Wea. Rev.* **117,** 536–549.

Ookouchi Y., Segal M., Kessler R. C. and Pielke R. A. (1984) Evaluation of soil moisture effects on the generation and modification of mesoscale circulations. *Mon. Wea. Rev.* **112,** 2281–2292.

Orlanski I. (1976) A simple boundary condition for unbounded hyperbolic flows. *J. Comput. Phys.* **21,** 251–269.

Pielke R. A. (1984) *Mesoscale Meteorological Modelling.* Academic Press, New York, 612 pp.

Pielke R. A., Dalu G. A., Snook J. S., Lee T. J. and Kittel T. G. F. (1991) Nonlinear influence of mesoscale land use on weather and climate. *J. Clim.* **4,** 1053–1069.

Pinty J.-P., Mascart, P., Richard E. and Rosset R. (1989) An investigation of mesoscale flows induced by vegetation inhomogeneities using an evapotranspiration model calibrated against HAPEX-MOBILHY data. *J. appl. Met.* **28,** 976–992.

Raupach M. R. and Finnigan J. J. (1988) Single-layer models of evaporation are incorrect but useful, whereas multilayer models are correct but useless. *Aust. J. Plant Physiol.* **15,** 705–716.

Rutledge S. A. and Hobbs P. V. (1983) The mesoscale and microscale structure and organization of clouds and precipitation in midlatitude cyclone. VIII: A model for the "seeder-feeder" process in warm-frontal rainbands. *J. atmos. Sci.* **40,** 1185–1206.

Segal M. and Avissar R. *et al.* (1988) Evaluation of vegetaion effects on the generation and modification of mesoscale circulations. *J. atmos. Sci.* **45,** 2268–2292.

Smith R. B. and Lin Y.-L. (1982) The addition of heat to a stratified airstream with application to the dynamics of orographic rain. *Q. J. R. met. Soc.* **108,** 353–378.

Sun W.-Y. (1981a) Large mesoscale convection and sea breeze circulation. Part I: linear stability analysis. *J. atmos. Sci.* **38,** 1675–1693.

Sun W.-Y. (1981b) Large mesoscale convection and sea breeze circulation. Part I: nonlinear numerical model. *J. atmos. Sci.* **38,** 1694–1706.

Tjerström M. (1989) Some tests with a surface energy balance scheme, including a bulk parameterisation for vegetation, in a mesoscale model. *Boundary-Layer Met.* **48,** 33–68.